Available online at www.sciencedirect.com
SCIENCE DIRECT®
Carbohydrate Research 340 (2005) 2185–2194
Carbohydrate RESEARCH

QM/MM study of D-fructose in aqueous solution

Marília T. C. Martins Costa*

Equipe Chimie et Biochimie Théoriques, UMR CNRS-Université Henri Poincaré, Nancy I no. 7565, BP 239, 54506 Vandoeuvre-lès-Nancy, F-54506 France

Received 27 September 2004; received in revised form 23 June 2005; accepted 23 June 2005
Available online 20 July 2005

Abstract—The QM/MM molecular dynamics methodology was applied to the study of the two main D-fructose tautomers present in aqueous solution, β-D-fructofuranose and β-D-fructopyranose. The solute was treated at the AM1 semi-empirical level, and for the solvent water molecules we used the TIP3P potential. We analyzed the structure of the water molecules around the hydroxyl groups to explain the differences in sweet taste between the two tautomers.

Keywords: D-Fructose; Solvent effect; QM/MM molecular dynamics; Sweet taste

1. Introduction

The only crystalline form of D-fructose, β-D-fructopyranose,[1,2] is known to be about twice as sweet as sucrose. However, in aqueous solution, where the two main tautomers present are β-D-fructofuranose and β-D-fructopyranose,[3–6] sweetness is considerably diminished.[7] From this observation, one can predict that the furanoid form is substantially less sweet than the pyranoid form, or not sweet at all.[8]

Consequently, interpretation of fructose sweetness is based on the β-pyranoid form. Shallenberger, Acree[9] and Kier[10] tried to explain the sweet taste via the existence of an AH–B–γ glucophore unit, and several possible glucophores have been proposed in the case of D-fructose. Shallenberger and Lindley[11] identified the OH-2–O-1–C-6 glucophore unit. Mathlouthi and Portmann[12] made the inverse assignment: OH-1–O-2–C-6. Birch et al.[13] concluded at the OH-3–O-4–C-6 or OH-4–O-3–C-6 assignment. Lichtenthaler and Immel[14] arrived at the same conclusion regarding the hydrophilic AH–B part, but the hydrophobic γ part would be an entire region rather than a specific corner, located opposite to the hydrophilic region and reaching from CH_2-1 to CH_2-6 (see Fig. 1). All these assignments are particular cases of the more general multipoint attachment theory proposed by Nofre and Tinti,[15] that assumes the presence of four hydrogen bond acceptor sites.

Fructose theoretical calculations available in the literature concern mainly conformational studies in gas phase, using various levels of approximation.[16–23] The major role of water–sugar interactions on the sweetness of the most common nutritive sugars has been emphasized by various studies.[24–29] It is therefore particularly important to consider the solvent explicitly in the calculations. Molecular dynamics simulations using classical force fields have been widely applied to aqueous solutions of different carbohydrates,[30] but are scarce for fructose.[31,32] While classical force fields may be sufficient to represent the solvent, the carbohydrate molecules, which contain highly polarized groups, are not accurately described.[33] This shortcoming is overcome with the use of hybrid quantum mechanics/molecular mechanics (QM/MM) potentials,[34–38] in which the solute molecule is treated with a quantum mechanical method and the solvent with an empirical potential.

In this study, we applied the QM/MM molecular dynamics methodology in order to get a deeper insight on the behaviour of carbohydrates in aqueous solution.

* Tel.: +33 383 684376; fax: +33 383 684371; e-mail: marilia.martins-costa@cbt.uhp-nancy.fr

0008-6215/$ - see front matter © 2005 Elsevier Ltd. All rights reserved.
doi:10.1016/j.carres.2005.06.020

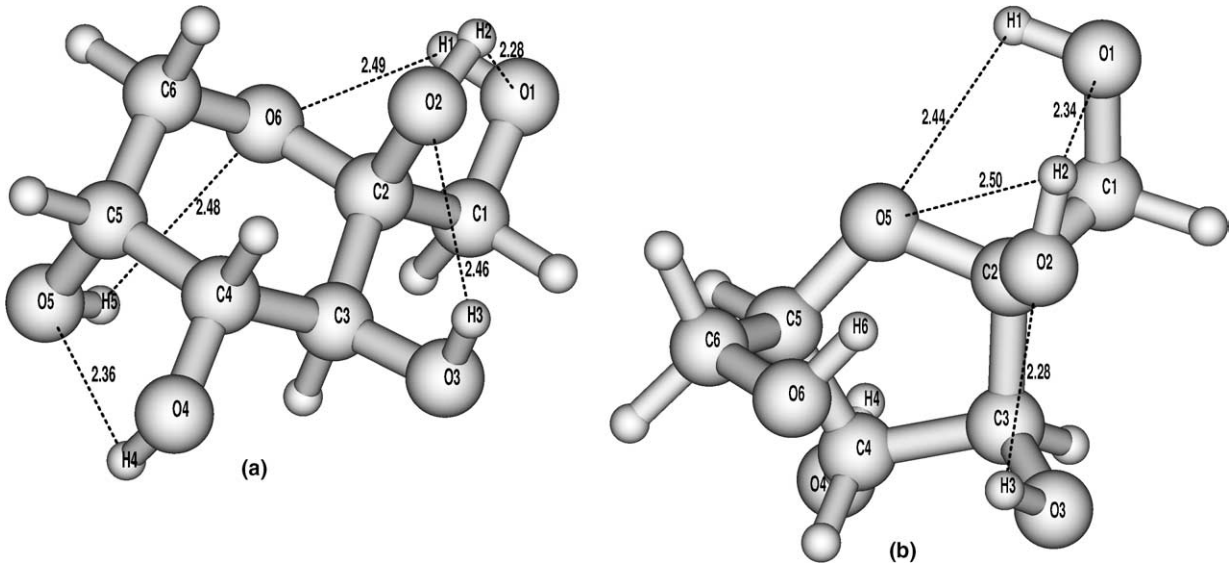

Figure 1. Minimum-energy gas phase AM1 structures of (a) β-D-fructopyranose and (b) β-D-fructofuranose.

We treated β-D-fructofuranose and β-D-fructopyranose quantum mechanically at the AM1 semi-empirical level,[39,40] which is well adapted to the study of monosaccharides.[20,21,41] The solvent is composed of TIP3P classical water molecules.[42] We tried to interprete the differences in sweetness in terms of different behaviours of the two tautomers towards water.

2. Computational methodology

The system is composed of the solute molecule treated quantum mechanically (QM region) at the AM1 semi-empirical level,[39,40] and 512 water molecules described by molecular mechanics (MM region) using the TIP3P potential.[42] The whole system is placed inside a cubic box of 25 Å with periodic boundary conditions.

The QM/MM interaction involves an electrostatic term that depends on the QM electrons, and therefore must be included in the HF-SCF iterative procedure. For the electrostatic interaction between the MM atoms and the QM nuclei, we used the AM1 repulsive function for consistency. We used a Lennard–Jones potential for the QM/MM van der Waals contribution with, for the QM atoms, the optimized Lennard–Jones parameters proposed by Gao.[43]

MD simulations were made in the NVE ensemble. The equations of motion were numerically integrated using the Verlet algorithm for the solute and the quaternion based algorithm of Fincham for the rigid solvent molecules.[44] The target temperature was 298 K, and velocities were scaled every 200 time steps to avoid small systematic drifts. A smooth truncation function was applied to the solvent–solvent and solute–solvent interactions.[45]

After an equilibration period of 100 ps, the average collection was performed for a period of 500 ps. The

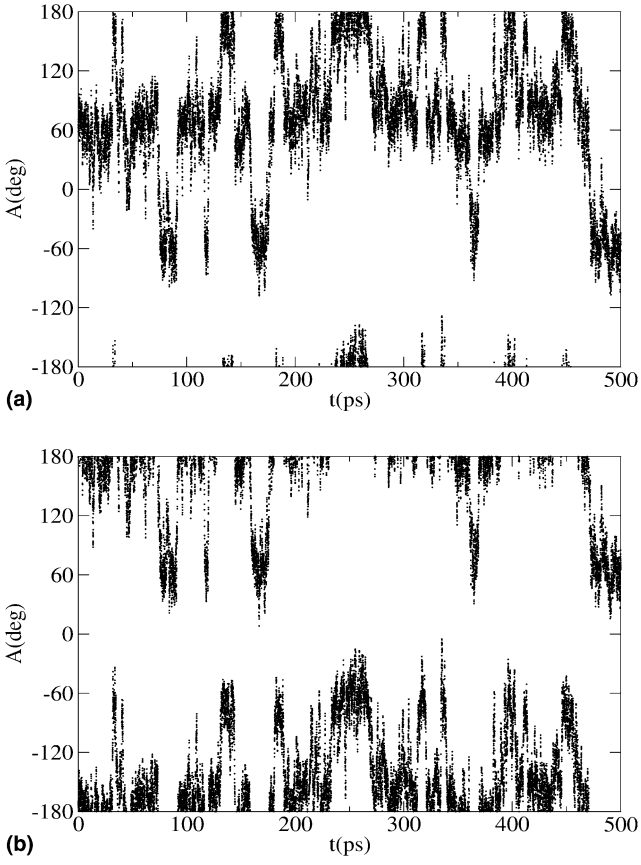

Figure 2. History of the β-D-fructopyranose primary alcohol group orientation in aqueous solution: (a) O-1–C-1–C-2–O-5 and (b) O-1–C-1–C-2–C-3.

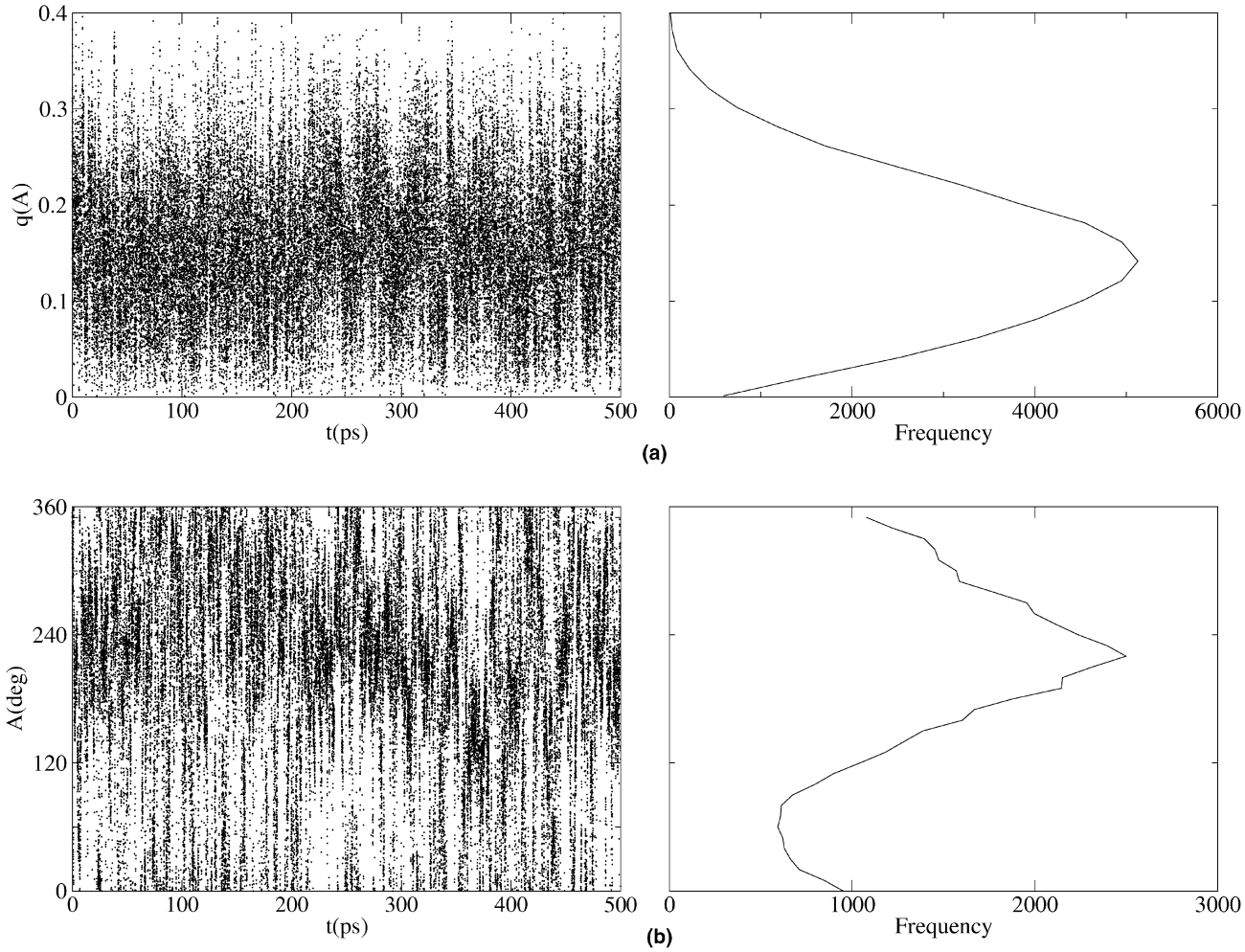

Figure 3. History of the β-D-fructofuranose Cremer–Pople puckering parameters in aqueous solution and corresponding histograms, computed with bin widths of 0.02 Å and 10°: (a) q and (b) ϕ.

time step was 0.5 fs, and configurations were saved every 10 fs for further analysis.

All calculations were done with the CHIMISTE/MM package.[†]

3. Results and discussion

3.1. Conformational analysis

We first carried out a conformational search at the AM1 level on each isolated molecule, using high temperature molecular dynamics in gas phase. The temperature was set to 600 K, and 1000 structures saved from a 100 ps simulation were then minimized. In Figure 1, the AM1 minimum energy conformations found are presented. β-D-Fructopyranose (FP) adopts the $^2C_5$ conformation, with a *GT* orientation of the hydroxymethyl O-1–C-1 bond with respect to the ring C-2–O-5 and C-2–C-3 bonds. β-D-Fructofuranose (FF) has a *GG* orientation of the hydroxymethyl O-6–C-6 bond relative to the ring C-5–O-5 and C-5–C-4 bonds and a *GT* orientation of the hydroxymethyl O-1–C-1 bond relative to the ring C-2–O-5 and C-2–C-3 bonds, and a ^5E ring orientation,[46] but 12 other conformations were found within 2 kcal/mol of the global minimum, in agreement with ab initio and molecular mechanics results.[23,18]

In aqueous solution, β-D-fructopyranose was always observed in the $^2C_5$ conformation. The *GT* orientation of the hydroxymethyl O-1–C-1 bond was still the most favoured one, occurring for about 60% of the simulation time, with the *GG* and the *TG* orientations equally

[†]M. T. C. Martins Costa and C. Millot, CHIMISTE/MM, Université Henri Poincaré-Nancy I, 1996. This program performs classical Monte Carlo and molecular dynamics simulations of systems composed of a subsystem described at a semi-empirical level and discrete classical solvent molecules interacting through a pairwise additive intermolecular potential.

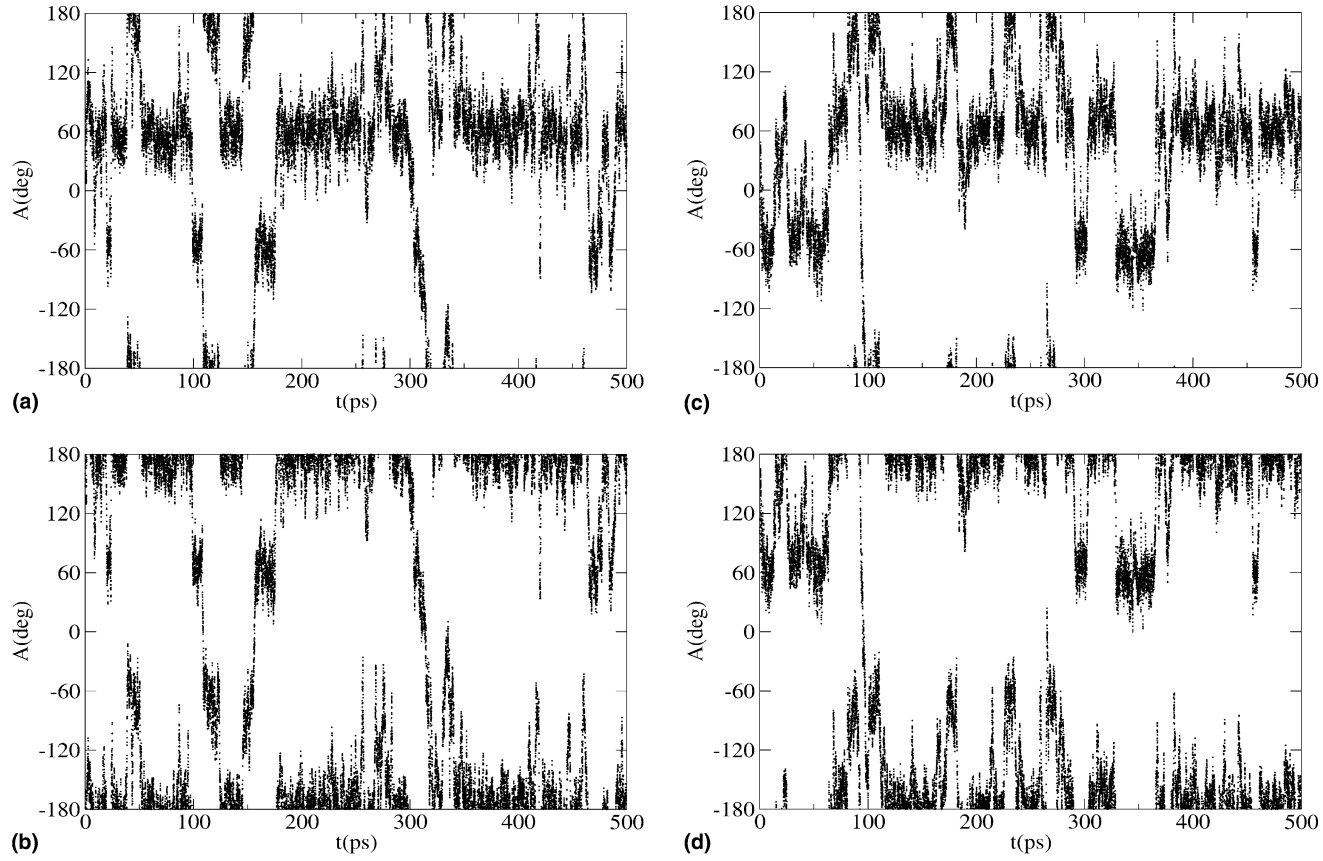

Figure 4. History of the β-D-fructofuranose primary alcohol group orientations in aqueous solution: (a) O-1–C-1–C-2–O-5, (b) O-1–C-1–C-2–C-3, (c) O-6–C-6–C-5–O-5 and (d) O-6–C-6–C-5–C-4.

Table 1. β-D-Fructopyranose and β-D-fructofuranose optimized gas phase atomic charges and corresponding average values and mean absolute deviations in aqueous solution, in au

	β-D-Fructopyranose		β-D-Fructofuranose	
	Gas phase	Solution	Gas phase	Solution
O-1	−0.324	−0.376 ± 0.021	−0.322	−0.376 ± 0.022
O-2	−0.348	−0.384 ± 0.023	−0.336	−0.377 ± 0.023
O-3	−0.301	−0.365 ± 0.021	−0.293	−0.357 ± 0.021
O-4	−0.303	−0.374 ± 0.021	−0.302	−0.367 ± 0.023
O-5	−0.322	−0.376 ± 0.022	−0.318	−0.326 ± 0.022
O-6	−0.316	−0.319 ± 0.022	−0.337	−0.389 ± 0.020

Table 2. β-D-Fructopyranose and β-D-fructofuranose optimized gas phase intramolecular hydrogen bond lengths, corresponding average values and mean absolute deviations in aqueous solution, in Å

	β-D-Fructopyranose		β-D-Fructofuranose	
	Gas phase	Solution	Gas phase	Solution
H-1···O-2	3.08	3.03 ± 0.44 (16)	3.11	3.03 ± 0.47 (21)
H-1···O-5			2.44	3.10 ± 0.48 (17)
H-1···O-6	2.49	3.16 ± 0.47 (33)		
H-2···O-3			3.50	2.92 ± 0.44 (25)
H-2···O-5			2.50	2.43 ± 0.18 (68)
H-2···O-6	2.55	2.51 ± 0.17 (56)		
H-2···O-1	2.28	2.90 ± 0.51 (33)	2.34	3.34 ± 0.52 (14)
H-3···O-2	2.46	2.63 ± 0.33 (51)	2.28	2.58 ± 0.31 (52)
H-4···O-5	2.36	2.61 ± 0.36 (56)		
H-5···O-6	2.48	2.82 ± 0.33 (22)		
H-6···O-5			2.61	3.11 ± 0.49 (18)

In parentheses, the percentage of simulation time where the H···O distances were less than 2.5 Å. Only values greater than 10% were retained.

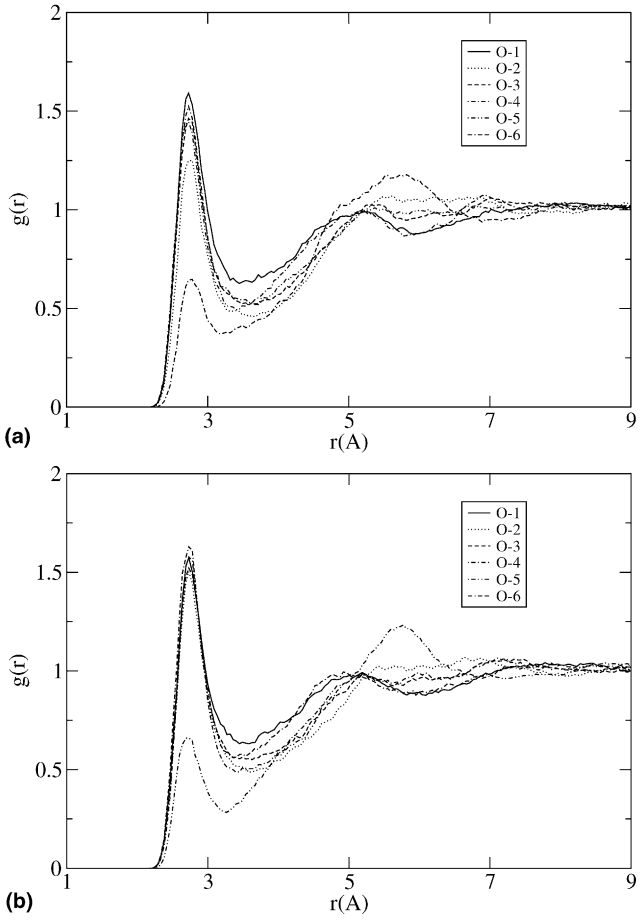

Figure 5. Radial distribution functions of β-D-fructopyranose and β-D-fructofuranose oxygen atoms with respect to the oxygen water atom: (a) β-D-fructopyranose and (b) β-D-fructofuranose.

Table 3. Coordination numbers from the radial distribution functions of β-D-fructopyranose and β-D-fructofuranose oxygen atoms with respect to the water oxygen atom

	O-1	O-2	O-3	O-4	O-5	O-6
β-D-Fructopyranose	3.66	2.80	3.24	3.35	3.14	1.68
β-D-Fructofuranose	3.58	3.24	3.36	3.21	1.57	3.49

present for the rest of the time, and many transitions between the different orientations. The history of the corresponding dihedral angles is presented in Figure 2.

The β-D-fructofuranose tautomer is highly flexible in aqueous solution, with many ring orientations populated. The preferred ones are in the north–west zone, mainly in the ^{2}E–$^{2}_{3}T$–$_{3}E$–$^{4}_{3}T$ zone, and in the south–west zone near the gas phase global minimum ^{5}E. The history of the Cremer–Pople parameters[46] is shown in Figure 3. Our calculations predict that furanose rings are much less puckered than those obtained by molecular mechanics,[22] but also less puckered than those found in most crystal structures. The gas-phase conformations within 2 kcal/mol of the global minimum have values in the same range, and the solvent effect is thus quite low. Our results seem to follow the general trend of AM1 that underestimates furanose puckering.[47] The two primary alcohol groups adopted preferably the *GT* orientation (Fig. 4).

3.2. Mulliken charges

Polarization effects in aqueous solutions of carbohydrate molecules are important, due to the presence of several hydroxyl groups. Being highly flexible, these effects will produce conformational variations of the atomic charges that are not taken into account by fixed charge force fields traditionally used. Ignoring these variations can lead to serious errors.[48] The QM/MM potentials allow polarization of the solute wavefunction in the presence of the solvent partial charges, and we can estimate these polarization effects by comparing the atomic Mulliken charges in aqueous solution to gas phase values. This is done in Table 1 for the oxygen atoms of the fructose tautomers studied.

There is almost no effect of water on the ring oxygens, and the largest effect lies in the O-3–O-4 region in both cases. There is a non-uniform polarization in solution, up to 23%.

Table 4. Average number of hydrogen bonds, hydrogen bond distances (in Å) and angles (in °) between water and hydroxyl groups in aqueous solutions of β-D-fructopyranose and β-D-fructofuranose

	β-D-Fructopyranose				β-D-Fructofuranose			
	⟨HB⟩	⟨O–O⟩	⟨O···H⟩	⟨O–O–H⟩	⟨HB⟩	⟨O–O⟩	⟨O···H⟩	⟨O–O–H⟩
O-1	1.36	2.86	2.06	9.2	1.42	2.86	2.06	9.1
O-2	0.88	2.87	2.08	9.5	1.22	2.88	2.08	9.4
O-3	1.27	2.86	2.06	9.1	1.26	2.87	2.06	9.0
O-4	1.43	2.85	2.04	8.7	1.26	2.85	2.02	8.0
O-5	1.22	2.84	2.02	8.5				
O-6					1.49	2.84	2.02	8.3
H-1	0.92	2.97	2.15	9.0	0.90	2.98	2.16	9.0
H-2	0.89	2.93	2.10	8.2	0.86	2.92	2.09	8.5
H-3	0.82	2.97	2.14	8.2	0.89	2.94	2.10	7.9
H-4	0.79	2.98	2.15	8.7	0.95	2.91	2.06	7.3
H-5	0.79	2.92	2.11	9.7				
H-6					0.88	2.96	2.13	8.9

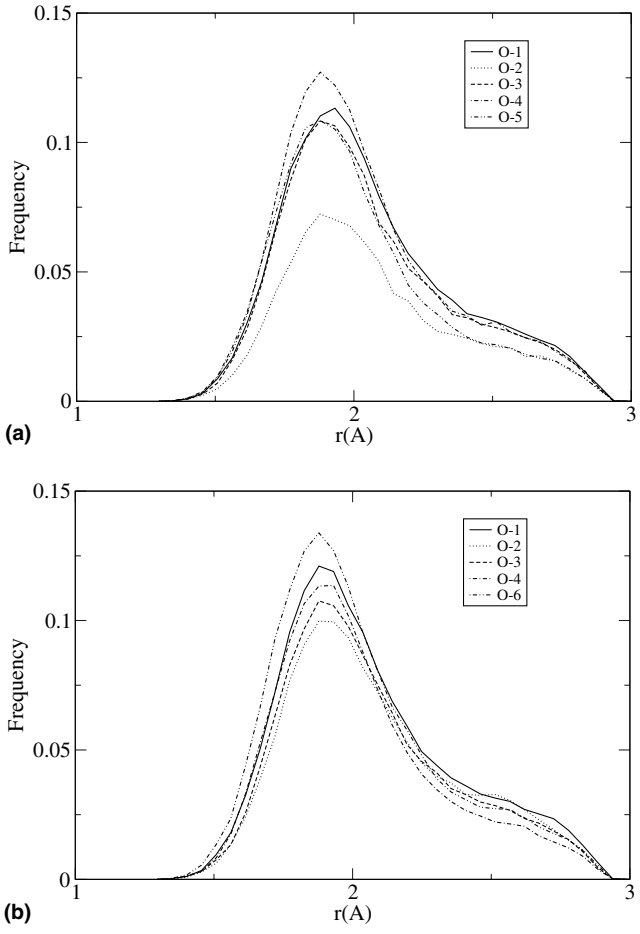

Figure 6. Histogram (0.05 Å bin width) of the acceptor hydrogen bond distance O–H for the β-D-fructopyranose and β-D-fructofuranose hydroxyl groups: (a) β-D-fructopyranose and (b) β-D-fructofuranose.

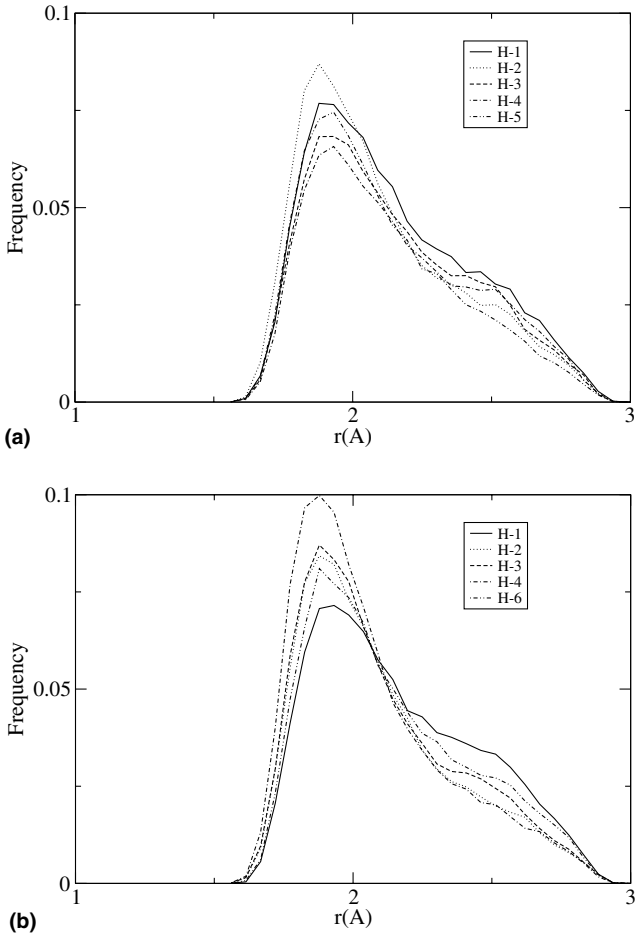

Figure 7. Histogram (0.05 Å bin width) of the donor hydrogen bond distance H–O for the β-D-fructopyranose and β-D-fructofuranose hydroxyl groups: (a) β-D-fructopyranose and (b) β-D-fructofuranose.

3.3. Intramolecular hydrogen bond network

In gas phase, there are networks of weak intramolecular hydrogen bonds, also present in crystal structures,[1,2] molecular mechanics[22] and ab initio calculations.[23] Gas phase hydrogen bond distances, as well as averaged values in solution, are summarized in Table 2.

The intramolecular hydrogen bonds, although weakened relative to gas phase in general, are present in aqueous solution to a significant extent. Taking an H···O distance of 2.5 Å as cutoff, seven intramolecular hydrogen bonds are found in solution during more than 10% of the simulation time. Strong interactions occur between H-2 and the ring oxygen atom, and between O-2 and H-3 in both FF and FP. H-2 participates during all the simulation time in a weak hydrogen bond with one of its oxygen neighbours: O-1, the ring oxygen, but also with O-3 in the case of FF. The most significant difference between the two forms is H-4 that participates in a weak hydrogen bond with its neighbour O-5 in FP for about half of the simulation time, but not in FF.

3.4. Intermolecular hydrogen bond network

The radial distribution functions of fructose oxygen atoms with respect to the solvent oxygen atom are shown in Figure 5, and the corresponding cooordination numbers are given in Table 3. The solvation of the ring oxygen is quite different from that of the hydroxyl oxygens. For both tautomers, much less water is found in its vicinity.

The other FF values are divided into two groups. The hydroxymethyl oxygen atoms O-1 and O-6 have the highest coordination numbers, and all the other hydroxyl oxygen atoms have similar values between 3.2 and 3.4. For FP, the hydroxymethyl oxygen O-1 has also the highest coordination number. O-3, O-4 and O-5 have values similar to the FF hydroxyl oxygen atoms, and a particularly low value occurs for the anomeric oxygen atom.

The coordination numbers give only a rough idea of the solute–solvent interactions, as far as not all the water molecules within the first solvation shell are hydrogen bonded to the hydroxyl atoms. To make such an analysis, we used as criteria an O–O distance of less than

3.5 Å and an O···H–O angle greater than 120°, as proposed before.[31,49] We found significant differences between the two tautomers. The results are summarized in Table 4. In Figures 6 and 7, the histograms of the acceptor and donor hydrogen bond distances are depicted. For FF, the hydroxymethyl oxygens O-1 and O-6 have the highest average number of hydrogen bonds. O-2, O-3 and O-4 have similar values. For FP, we have two good acceptors, O-1 and O-4, but O-4 forms stronger and better oriented acceptor hydrogen bonds. The anomeric group OH-2 is a poor acceptor of hydrogen bonds in FP. In FF, OH-4 is the best donor of hydrogen bonds. The other hydroxyl groups are also good donors. The hydroxymethyl groups in both tautomers form very weak donor hydrogen bonds. For FP, the anomeric group OH-2 is also a good donor, and the other hydroxyl groups are poor donors.

3.5. Intermolecular hydrogen bond dynamics

In order to analyze the behaviour of the water molecules around the hydroxyl groups, we computed autocorrelation functions of several population operators (Eq. 1)

$$\langle \hat{h}(t)\hat{h}(0)\rangle / \langle \hat{h}(0)\hat{h}(0)\rangle \quad (1)$$

where $\hat{h}$ is a binary operator.[50–52] The first shell water residence population operator around each hydroxyl group is assigned the value of one when the hydroxyl oxygen–water oxygen distance is less than 3.5 Å, and zero otherwise. The hydrogen bond acceptor or donor population operators have a value of one when a water molecule is hydrogen bonded to the oxygen or the hydrogen of the hydroxyl group, respectively, and zero otherwise. We estimated the water residence time and the hydrogen bond acceptor and donor lifetimes from the integral of these functions, calculated numerically up to 10 ps, and from a fit to an exponential decay at larger times.[53] The results are depicted in Figures 8–10 and summarized in Tables 5 and 6.

The water mobility is slightly higher around the hydroxymethyl groups, as they have a greater

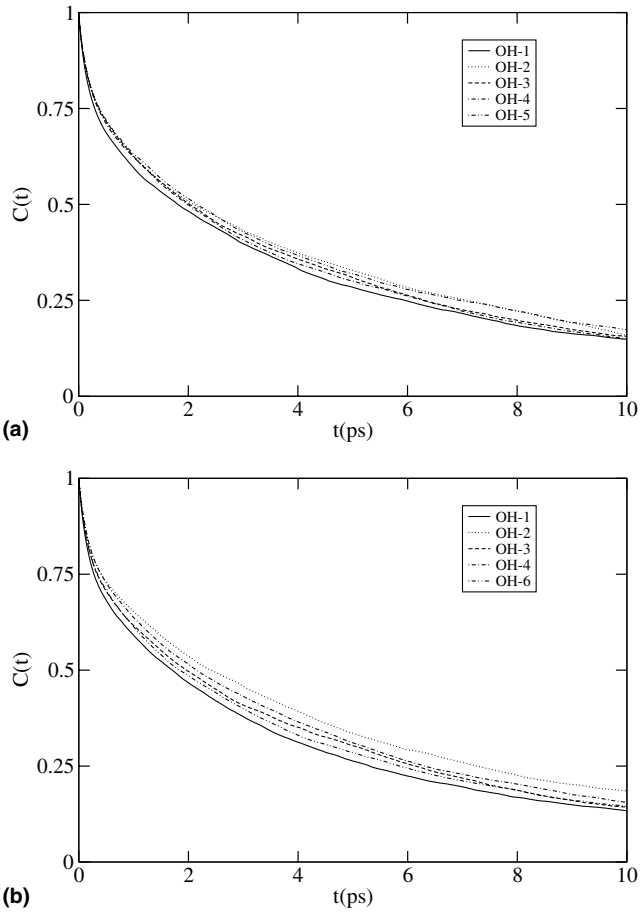

Figure 8. Autocorrelation function of the water residence population operator around the β-D-fructopyranose and β-D-fructofuranose hydroxyl groups: (a) β-D-fructopyranose and (b) β-D-fructofuranose.

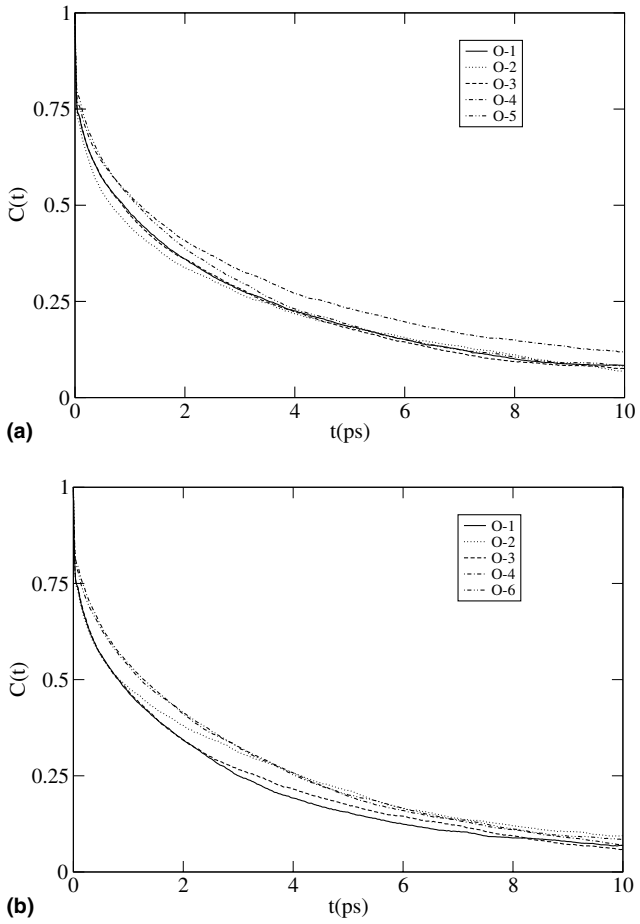

Figure 9. Autocorrelation function of the acceptor hydrogen bond population operator around the β-D-fructopyranose and β-D-fructofuranose hydroxyl groups: (a) β-D-fructopyranose and (b) β-D-fructofuranose.

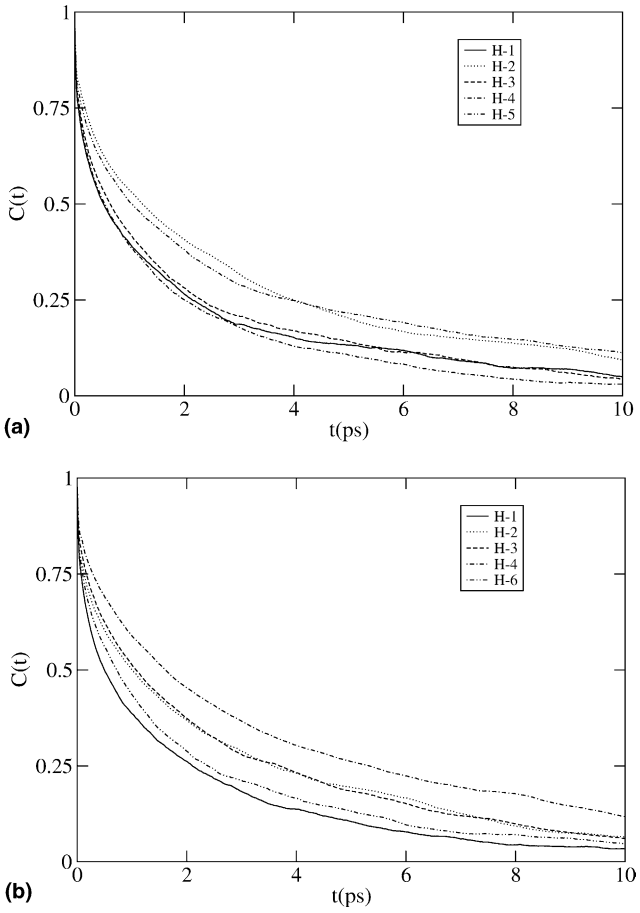

Figure 10. Autocorrelation function of the donor hydrogen bond population operator around the hydroxyl groups of β-D-fructopyranose and β-D-fructofuranose: (a) β-D-fructopyranose and (b) β-D-fructofuranose.

accessibility to the solvent. In FF, the water residence time around OH-2 is greater than around the other groups, whose values are comprised between 4.1 and 4.6 ps. All FP values are similar, comprised between 4.4 and 5.0 ps.

Table 5. Water residence lifetimes (in ps) around hydroxyl groups in aqueous solutions of β-D-fructopyranose and β-D-fructofuranose

	OH-1	OH-2	OH-3	OH-4	OH-5	OH-6
β-D-Fructopyranose	4.4	4.8	4.6	4.5	5.0	
β-D-Fructofuranose	4.1	5.2	4.4	4.6		4.4

Table 6. Lifetimes (in ps) of the hydrogen bonds between water and hydroxyl groups in aqueous solutions of β-D-fructopyranose and β-D-fructofuranose

	O-1	O-2	O-3	O-4	O-5	O-6
β-D-Fructopyranose	2.8	2.7	2.7	3.6	3.0	
β-D-Fructofuranose	2.6	3.1	2.6	3.0		3.1
	H-1	H-2	H-3	H-4	H-5	H-6
β-D-Fructopyranose	2.1	3.4	2.1	1.7	3.5	
β-D-Fructofuranose	1.8	2.7	2.7	4.0		2.1

Looking now at Table 6, one can see that the highest acceptor hydrogen bond lifetime occurs for OH-4 in FP. All the other values are similar in both tautomers. Concerning the donor hydrogen bond lifetimes, the greatest difference comes again from the OH-4 group, with the lowest value in FP and the highest value in FF.

3.6. Bridged water molecules

Another interesting feature of aqueous solutions of carbohydrates is the occurrence of bridged water molecules between two adjacent hydroxyl group atoms. This was found in several molecular dynamics studies of similar systems.[26,54,55] The results in Table 7 are obtained by counting the water molecules simultaneously hydrogen bonded to one hydroxyl atom and to another hydroxyl atom or to the ring oxygen. In Table 8 and in Figure 11, FP and FF results for specific pair of atoms or

Table 7. Simulation time (in %) of one water molecule was hydrogen bonded to one specific QM atom and any other QM atom

	O-1	O-2	O-3	O-4	O-5	O-6
β-D-Fructopyranose	40	47	41	35	25	44
β-D-Fructofuranose	45	74	31	6	70	34
	H-1	H-2	H-3	H-4	H-5	H-6
β-D-Fructopyranose	34	27	30	17	16	
β-D-Fructofuranose	30	54	37	6		28

Table 8. Simulation time (in %) of one bridged water molecule was found between two QM atoms

	O-1–O-2	O-1–O-5	O-1–O-6	O-2–O-3	O-2–O-5	O-5–O-6
β-D-Fructopyranose	10		16			
β-D-Fructofuranose	16	16		21	17	18
	O-3–O-4	O-2–H-3	O-5–H-1	H-2–H-3	H-1–H-2	
β-D-Fructopyranose	22	18			16	
β-D-Fructofuranose			16	25		

Only values greater that 10% were retained.

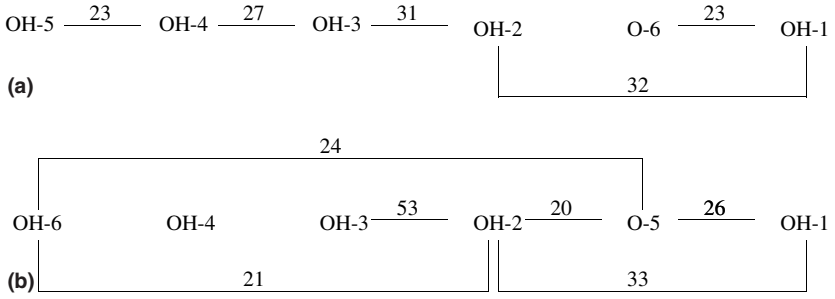

Figure 11. Schematic representation of bridged water molecules (in % of simulation time) around β-D-fructopyranose and β-D-fructofuranose hydroxyl groups: (a) β-D-fructopyranose and (b) β-D-fructofuranose.

groups are compared. The most significant difference comes from OH-4 that shares one water molecule with its neighbours for about half of the simulation time in FP, the highest value occurring between O-3 and O-4. In FF, O-4 and H-4 rarely share water molecules with their hydroxyl neighbours, and O-3 prefers the anomeric oxygen O-2 to O-4. The anomeric group OH-2 in FF shares one water molecule with its neighbours OH-1 and OH-3, with the ring oxygen, but also with OH-6. In FP, OH-2 is much less involved in the intermolecular hydrogen bond network.

4. Conclusions

We have performed QM/MM molecular dynamics simulations of aqueous solutions of β-D-fructopyranose (FP) and β-D-fructofuranose (FF), and analyzed the different behaviours of these tautomers towards water.

Water was found to play an important role in the accessibility of many areas of the conformational space, particularly in the case of FF. The polarization effects in aqueous solution lead to non-uniform variations of the oxygen atomic charges, particularly important in the O-3–O-4 region.

With regard to intermolecular hydrogen bonding capabilities, the greatest difference came from the OH-4 group, which behaves as the best acceptor and the worst donor of hydrogen bonds in FP, the opposite trend being predicted in FF. Indeed, our results indicate a region with a marked hydrophilic character behaviour around OH-3 and OH-4 in FP. This behaviour is less important in FF, as OH-4 exhibits a poorer hydrogen bond acceptor capability. Besides, our calculations for FP show that the worst hydrogen bond acceptor is OH-2. This reinforces the hydrophobic character of the CH_2-1–CH_2-6 region that could then be the γ component of the glucophore sweet taste unit, as proposed by Lichtenhaler and Immel.[14] In FF, the hydrophobicity of this region is largely reduced due to the presence of good hydrogen bond acceptors OH-1, OH-2 and OH-6. For FP, the AH–B component would then be OH-3–O-4, in agreement with the assignments of Birch et al.[13] The poor hydrogen bond acceptor capability of OH-4 in FF does not allow it to have such a good hydrophilic region.

The importance of the OH-4 group with respect to structure–sweetness relationships, already emphasized by other studies,[14,16,56] is confirmed. Its particularly good hydrogen bond acceptor character in FP might be related to cooperative effects, as far as the existence of an intramolecular hydrogen bond between H-4 and O-5 enhances the basicity of O-4. The H-3–O-2 intramolecular hydrogen bond, implying that H-3 is turned to the opposite side with respect to O-4, should also contribute to the larger hydrogen bond acceptor character of OH-4 in FP. A water molecule is present in the region between O-3 and O-4 for about 25% of the simulation time in FP. In FF, O-3 is intramolecularly hydrogen bonded to H-2 for 25% of the simulation time, and thus less involved in the hydrogen bond network with water. The intramolecular/intermolecular hydrogen bond balance in the OH-3–OH-4–OH-5 and OH-1–O-6–OH-2 regions in FP, and OH-3–OH-4–OH-6 and OH-1–O-5–OH-2 in FF, is quite different, and could explain the difference in sweet taste of the two tautomers.

References

1. Kanters, J. A.; Roelofsen, G.; Alblas, B. P.; Meinders, I. *Acta Crystallogr. B* **1977**, *33*, 665–672.
2. Takagi, S.; Jeffrey, G. A. *Acta Crystallogr. B* **1977**, *33*, 3510–3515.
3. Hyvönen, L.; Varo, P.; Koivistoinen, P. *J. Food Sci.* **1977**, *42*, 652–653.
4. Hyvönen, L.; Varo, P.; Koivistoinen, P. *J. Food Sci.* **1977**, *42*, 654–656.
5. Lichtenthaler, F. W.; Rönninger, S. *J. Chem. Soc., Perkin. Trans. 2* **1990**, 1489–1497.
6. Flood, A. E.; Johns, M. R.; White, E. T. *Carbohydr. Res.* **1996**, *288*, 45–56.
7. Tsuzuki, Y.; Yamakazi, J. *Biochem. Z.* **1953**, *323*, 525–531.
8. Shallenberger, R. S. *Pure Appl. Chem.* **1978**, *50*, 1409–1420.
9. Shallenberger, R. S.; Acree, T. E. *Nature* **1967**, *216*, 480–482.
10. Kier, L. B. *J. Pharm. Sci.* **1972**, *61*, 1394–1397.

11. Shallenberger, R. S.; Lindley, M. G. *Food Chem.* **1977**, *2*, 145–153.
12. Mathlouthi, M.; Portmann, M. O. *J. Mol. Struct.* **1990**, *237*, 327–338.
13. Birch, G. G.; Shamil, S.; Shepherd, Z. *Experientia* **1986**, *42*, 1232–1234.
14. Lichtenthaler, F. W.; Immel, S. In *Sweet-Taste Chemoreception*; Mathlouthi, M., Kanters, J. A., Birch, G. G., Eds.; Elsevier Applied Science: London, 1993.
15. Nofre, C.; Tinti, J.-M. *Food Chem.* **1996**, *56*, 263–274.
16. Szarek, W. A.; Korppi-Tommola, S.-L.; Martin, O. R.; Smith, V. H., Jr. *Can. J. Chem.* **1984**, *62*, 1506–1511.
17. Woods, R. J.; Smith, V. H., Jr.; Szarek, W. A. *J. Chem. Soc., Chem. Commun.* **1987**, 937–939.
18. French, A. D.; Tran, V. *Biopolymers* **1990**, *29*, 1599–1611.
19. Garrett, E. C.; Serianni, A. S. *Carbohydr. Res.* **1990**, *206*, 183–191.
20. Woods, R. J.; Szarek, W. A.; Smith, V. H., Jr. *J. Am. Chem. Soc.* **1990**, *112*, 4732–4741.
21. Khalil, M.; Woods, R. J.; Weaver, D. F.; Smith, V. H., Jr. *J. Comput. Chem.* **1991**, *12*, 584–593.
22. French, A. D.; Dowd, M. K.; Reilly, P. J. *J. Mol. Struct. (Theochem.)* **1997**, *395–396*, 271–287.
23. Chung-Phillips, A.; Cheng, Y. Y. *J. Phys. Chem. A* **1999**, *103*, 953–964.
24. Mathlouthi, M. *Food Chem.* **1984**, *13*, 1–46.
25. Mathlouthi, M.; Seuvre, A.-M. *J. Chem. Soc., Faraday Trans. 1* **1988**, *84*, 2641–2650.
26. Brady, J. W.; Schmidt, R. K. *J. Phys. Chem.* **1993**, *97*, 958–966.
27. Mathlouthi, M.; Hutteau, F.; Angiboust, J. F. *Food Chem.* **1996**, *56*, 215–221.
28. Astley, T.; Birch, G. G.; Drew, M. G. B.; Rodger, P. M.; Wilden, G. R. H. *Food Chem.* **1996**, *56*, 231–240.
29. Birch, G. G. *Pure Appl. Chem.* **2002**, *74*, 1103–1108.
30. Imberty, A.; Pérez, S. *Chem. Rev.* **2000**, *100*, 4567–4588.
31. van Eijck, B. P.; Kroon-Batenburg, L. M. J.; Kroon, J. *J. Mol. Struct.* **1990**, *237*, 315–325.
32. Roberts, C. J.; Debenedetti, P. G. *J. Phys. Chem. B* **1999**, *103*, 7308–7318.
33. Hemmingsen, L.; Madsen, D. E.; Esbensen, A. L.; Olsen, L.; Engelsen, S. B. *Carbohydr. Res.* **2004**, *339*, 937–948.
34. Warshel, A.; Levitt, M. *J. Mol. Biol.* **1976**, *103*, 227–249.
35. Warshel, A. *J. Phys. Chem.* **1979**, *83*, 1640–1652.
36. Field, M. J.; Bash, P. A.; Karplus, M. *J. Comput. Chem.* **1990**, *11*, 700–733.
37. Gao, J. *Rev. Comput. Chem.* **1996**, *7*, 119–185.
38. Field, M. J. In *Computational Approaches to Biochemical Reactivity*; Naray-Szabo, G., Warshel, A., Eds.; Kluwer Academic Publishers: Dordrecht, 1997.
39. Dewar, M. J. S.; Storch, D. M. *J. Am. Chem. Soc.* **1985**, *107*, 3898–3902.
40. Dewar, M. J. S.; Zoebisch, E. G.; Healy, E. F.; Stewart, J. J. P. *J. Am. Chem. Soc.* **1985**, *107*, 3902–3909.
41. Woods, R. J.; Szarek, W. A.; Smith, V. H., Jr. *J. Chem. Soc., Chem. Commun.* **1991**, 334–337.
42. Jorgensen, W. L.; Chandrasekhar, J.; Madura, J. D.; Impey, R. W.; Klein, M. L. *J. Chem. Phys.* **1983**, *79*, 926–935.
43. Gao, J. *J. Phys. Chem.* **1992**, *96*, 6432–6439.
44. Allen, M. P.; Tildesley, D. J. *Computer Simulation in Liquids*; Clarendon Press: Oxford, 1987.
45. Brooks, B. R.; Burccoleri, R. E.; Olafson, B. D.; States, D. J.; Swaminatham, S.; Karplus, M. *J. Comput. Chem.* **1983**, *4*, 187–217.
46. Cremer, D.; Pople, J. A. *J. Am. Chem. Soc.* **1975**, *97*, 1354–1358.
47. Koole, L. H.; Neidle, S.; Krayevski, A. A.; Gurskaya, G. V.; Sandström, A.; Wu, J.-C.; Tong, W.; Chattopadhyaya, J. *J. Org. Chem.* **1991**, *56*, 6884–6892.
48. Reynolds, C. A.; Essex, J. W.; Richards, W. G. *Chem. Phys. Lett.* **1992**, *199*, 257–260.
49. Astley, T.; Birch, G. G.; Drew, M. G. B.; Rodger, P. M. *J. Phys. Chem. A* **1998**, *103*, 5080–5090.
50. Luzar, A.; Chandler, D. *Phys. Rev. Lett.* **1996**, *76*, 928–931.
51. Starr, F. W.; Nielsen, J. K.; Stanley, H. E. *Phys. Rev. Lett.* **1999**, *82*, 2294–2297.
52. Feenstra, K. A.; Hess, B. H.; Berendsen, H. J. C. *J. Comput. Chem.* **1999**, *20*, 786–798.
53. Koneshan, S.; Rasaiah, J. C.; Lynden-Bell, R. M.; Lee, S. H. *J. Phys. Chem. B* **1998**, *102*, 4193–4204.
54. Liu, Q.; Brady, J. W. *J. Am. Chem. Soc.* **1996**, *118*, 12276–12286.
55. Schmidt, R. K.; Brady, J. W. *J. Am. Chem. Soc.* **1996**, *118*, 541–546.
56. Pietrzycki, W. *Pol. J. Chem.* **2001**, *75*, 1569–1582.